Article

City Transmission Networks: Unraveling Disease Spread Dynamics

Hend Alrasheed [1,*] , Norah Alballa [2] , Isra Al-Turaiki [2] , Fahad Almutlaq [3] and Reham Alabduljabbar [1]

[1] Department of Information Technology, College of Computer and Information Sciences, King Saud University, Riyadh 11421, Saudi Arabia; rabduljabbar@ksu.edu.sa

[2] Department of Computer Science, College of Computer and Information Sciences, King Saud University, Riyadh 11421, Saudi Arabia; nalballa@ksu.edu.sa (N.A.); ialturaiki@ksu.edu.sa (I.A.-T.)

[3] Department of Geography, College of Humanities and Social Sciences, King Saud University, Riyadh 11451, Saudi Arabia; falmutlaq@ksu.edu.sa

* Correspondence: halrasheed@ksu.edu.sa

Abstract: In the midst of global efforts to curb the spread of infectious diseases, researchers worldwide are striving to unravel the intricate spatial and temporal patterns of disease transmission dynamics. Mathematical models are indispensable tools for understanding the dissemination of emerging pathogens and elucidating the evolution of epidemics. This paper introduces a novel approach by investigating city transmission networks as a framework for analyzing disease spread. In this network, major cities are depicted as nodes interconnected by edges representing disease transmission pathways. Subsequent network analysis employs various epidemiological and structural metrics to delineate the distinct roles played by cities in disease transmission. The primary objective is to identify superspreader cities. Illustratively, we apply this methodology to study COVID-19 transmission in Saudi Arabian cities, shedding light on the specific dynamics within this context. These insights offer valuable guidance for decision-making processes and the formulation of effective intervention strategies, carrying significant implications for managing public health crises.

Keywords: transmission network; epidemiological measures; structural measures; superspreader cities; COVID-19; GIS

1. Introduction

The transmission dynamics of infectious diseases are multifaceted, influenced by myriad factors such as demographic characteristics, population movements, host behaviors and immune responses, healthcare infrastructure, and environmental conditions [1,2]. Recent studies underscore that a minority of infected individuals, often termed superspreaders, can drive the majority of disease cases in an outbreak [3]. Furthermore, studies suggest that imported cases play a substantial role in seeding local transmission in various epidemic contexts, often accounting for a considerable proportion of total infections in many countries [4,5]. Interestingly, some cities exhibit characteristics that significantly influence the spread of diseases, similar to the role of individual superspreaders in an outbreak, prompting the adoption of the concept of superspreader cities[6]. Effective control strategies necessitate comprehensive measures, including both *within city* lockdowns and *between city* movement restrictions, to mitigate disease transmission rates [7].

Mathematically modeling disease transmission is a crucial step toward effective disease management, enabling better resource allocation in healthcare, the evaluation of control measures' effectiveness, and the prediction of transmission patterns. Epidemic modeling provides a potent tool for predicting the trajectory of an outbreak and devising strategies to contain it. Such models prove particularly useful in scenarios where data on mobility and travel are limited or inaccurate. Various mathematical modeling approaches have been employed in epidemiological contexts, including statistical models [8], mathematical formulations [9–11], and network-based analyses [12–14]. These models contribute

significantly to our understanding of disease dynamics and aid in developing evidence-based interventions for public health. However, most traditional epidemic models focus on the temporal aspect of the disease and are non-spatial [15]. While there are some studies that have successfully modeled disease spread within cities and among individuals [16–22], there remains a considerable gap in understanding and modeling between-city and cross-regional disease transmission.

In this study, we explore between-city transmission patterns utilizing a spatiotemporal network-based epidemic model. Spatiotemporal network-based epidemic models have been widely recognized and utilized in the field of epidemiology to study disease transmission dynamics, particularly in the context of infectious diseases. While there are various modeling approaches available, we choose the spatiotemporal network-based model due to its ability to capture both spatial and temporal dimensions of disease transmission patterns. It allows us to assess the role of different cities in the spread of a disease and identify potential superspreaders (cities with the highest potential to disseminate the disease). This highlights the critical importance of managing these influential nodes in disease control efforts [23,24].

Initially, we establish a city transmission network where nodes represent distinct cities and edges signify disease transmission from one city to another. Subsequently, the network is partitioned into multiple epidemic trees, each originating from a city with initial cases. These trees are then subjected to analysis using various epidemiological and structural metrics, offering quantitative insights for comparing the distinct roles cities play in disease propagation. Epidemiological measures delineate the spread of the epidemic among cities, while structural metrics scrutinize the static interconnectivity between them. Our approach emphasizes city connectivity over population size when studying disease propagation, recognizing that population size alone has limitations as a reliable predictor of disease spread [25].

We apply our framework to examine the case of COVID-19 in Saudi Arabia, leveraging authentic epidemiological data [26]. Our findings reveal that the impact of city infections is not confined to local boundaries but can extend across regional borders, affecting neighboring areas. Furthermore, we assert that the identification of superspreader cities holds greater significance than pinpointing infection sources. These results serve as valuable guidance for policymakers in setting priorities and refining quarantine strategies.

The rest of this work is organized as follows: Section 2 presents some preliminary concepts and definitions, and Section 3 presents the related work. Section 4 discusses the method, including network construction and analysis. Section 5 presents an illustrative example. Lastly, Section 6 concludes this paper.

2. Preliminaries

A crucial role in disease transmission is played by node accessibility (the local environment of the node) and reachability (the global environment of the node) within network structures [27–29]. Several network structures have been used to model disease propagation including social networks, contact networks, and disease transmission networks. In this work, we use the epidemic tree [15,30,31] structure to track disease transmission.

In graph theory, an *epidemic tree* $T_c = (V, E)$ rooted at node $c \in V$, where V is the set of nodes (infection cases) and E is the set of edges, is a directed rooted tree that allows understanding disease spread by its hidden structural properties [32]. The root of the tree c represents a primary case in the infection process.

Each tree edge represents a parent–child relationship in the disease spread process, where the parent node infects the child node. The creation of edges follows the chronological order of the infection of each pair of nodes such that a parent node is infected before its children nodes. The infection process from a parent node to a child node can be *deterministic* using node attributes such as the spatial distance to an infected parent node, or *stochastic* using probability [15,33–35].

An *epidemic forest* is a collection of epidemic trees which accrues when there are multiple primary cases. This representation assists the extraction of epidemic information at different spatial and temporal scales. It can also be used to reveal disease–environmental associations and guide disease control interventions.

The *neighborhood* of a node $u \in V$, denoted by $N(u)$, is the set of neighbors of u, i.e., $N(u) = v|u, v \in E$. The *degree* of node u is the size of its neighborhood ($d(u) = |N(u)|$). Node degrees have been shown to have a great impact on disease propagation [36,37].

A *path* in the tree connecting a pair of nodes u and v is a sequence of adjacent nodes that starts at u and ends with v. The *length* of a given path is the number of edges on the path. The *diameter* of a tree T_c, denoted by *diam* (T_c), is the number of nodes on a longest path between any two nodes in the tree. The tree diameter and average path length provide indications about the possibility of infection throughout the epidemic tree. For instance, the shorter the average path length between nodes, the higher the possibility of infection [28].

A *Breadth First Search* (BFS) starting at a given node u traverses the entire tree, level by level, by increasing distances from node u. That is, it starts traversing all nodes one hop away from u (u's neighbors). Then, it visits all nodes at two hops away from u, and so on. This systematic exploration helps in visualizing the spread and reach of potential infections across the network.

Node centrality measures rank nodes with respect to their importance by assigning a numerical value to each node according to its location in the network, which influences the overall dynamics of the network interactions. *Degree centrality* considers the central nodes to be those with the highest number of connections, highlighting potential hubs of activity or transmission. *Closeness centrality* identifies the center of the network as the subset of nodes with the shortest average distance to all other nodes, thereby highlighting those that can most efficiently spread or gather information, or, in the context of epidemics, transmit infections. In tree-structured networks, closeness centrality offers profound insights; the center, often referred to as the median and typically consisting of one or two nodes, is deemed the pivotal point of the network. This designation underscores its importance in strategic interventions and control measures. The application of closeness centrality is crucial for identifying key nodes, which are prioritized for thorough analysis and targeted in preventive strategies within epidemiological studies. This approach ensures that efforts are concentrated where they can be most effective in mitigating the spread of disease.

3. Related Work

Understanding how infections spread is crucial for controlling disease transmission. Epidemiology can greatly benefit from studying contact networks, as they provide valuable insights into disease propagation between individuals [12–14].

Recent studies have focused on utilizing advanced tools and methodologies to analyze city transmission networks and uncover hidden patterns of disease spread within cities. For instance, the study by John [38] investigated the impact of high connectivity and human movement on infectious disease transmission within city networks. The results indicated that travel time was the most crucial factor influencing disease transmission, followed by human movement. The study by Guo et al. [39] focused on a dynamic model of respiratory disease transmission by population mobility based on city networks, highlighting the importance of considering population mobility and disease transmission dynamics in urban settings. Leung et al. [40] conducted a systematic review on simulating contact networks for livestock disease epidemiology. The research altered the resulting network by randomly rewiring edges connecting node types that were not connected in the empirical network while preserving the clustering coefficient and mean degree of the Barabasi–Albert model simulation. This approach aimed to enhance the understanding of livestock disease transmission dynamics.

Luo et al. [29] studied COVID-19 transmission in the Chinese cities of Tianjin and Chengdu using visualization techniques, finding that transmission characteristics varied among cities. Büttner and Krieter [41] demonstrated various disease transmission routes

within animal trade networks, emphasizing the integration of different transmission pathways into simulation models. Xie et al. [42] investigated the impact of asymmetric activity on interactions between networks, highlighting the role of network structures. In a related study, Hearst et al. [43] identified potential superspreaders and disease transmission hotspots using white-tailed deer scraping networks. Krbylvik et al. [19] conducted network analysis of the detained and staff member movements in the Cook County Jail in Chicago, Illinois. The study, based on the movement of 5884 persons from 1 March to 30 April 2020, identified fewer COVID-19 links than expected among detained persons, implying that interventions and medical isolation policies were effective. In the networks of staff members, there were more links than predicted, indicating possible areas of concentration for further transmission.

Recent studies have also focused on the spatiotemporal dynamics of disease transmission. For instance, Shaw et al. [44] focused on modeling contacts and the spread of COVID-19 in the context of the return to work, demonstrating that limiting social contact through strategies such as reducing the number of people or time spent in the workplace are effective measures. Silva et al. [45] quantitatively analyzed the effectiveness of public health measures on COVID-19 transmission, emphasizing the importance of social isolation policies. Gayawan et al. [46] looked at the spatiotemporal dynamics of COVID-19 in 47 African countries. The study focused on the first 62 days of the disease's appearance in Africa, revealing that neighboring countries pose a major importation risk to each other. Chan and Wen [47] examined the impact of changes in intercity passenger rail travel on COVID-19 early spatial transmission in mainland China, investigating the association between structural changes in the railway origin-destination network and the prevalence of COVID-19 cases using Bayesian multivariate regression. Dlamini et al. [48] integrated various variables to spatially model COVID-19 transmission risk in Eswatini, analyzing case data for the period under strict lockdown. Pribadi et al. [49] studied the policy of Large-Scale Social Restriction (LSSR) in Jakarta, Indonesia, using hotspot analysis and space–time scan statistics to examine infection and transmission risk. The results suggest that spatial transmission continues despite a decrease in the overall pandemic curve during LSSR adoption.

In the context of Saudi Arabia, which serves as the case study for this work, the majority of COVID-19 research primarily focuses on statistical and mathematical models [50–56]. However, there is an opportunity to explore network-based approaches to better understand city-to-city disease transmission. While existing studies have utilized network-based SIR models [13], they often overlook the spatiotemporal aspect of the infection. Consequently, in this work, we propose a spatiotemporal network-based model to shed light on the dynamics of city-to-city disease transmission in Saudi Arabia.

4. Methods

We investigate between-city disease transmission patterns by analyzing city transmission networks. To achieve this goal, we initially build a city transmission network using data on infection and disease importation history. Subsequently, we conduct a quantitative analysis of the network's global, epidemiological, and structural characteristics.

4.1. Transmission Network Construction

To understand the dynamics of disease transmission across cities, we establish a city transmission network characterized by three fundamental components: central nodes denoting cities with initial imported cases (patient zero), nodes representing the remaining cities, and edges indicating the direction of transmission from one city to another. All central nodes are considered infected because they host at least one individual who contracted the disease while traveling. The remaining cities become infected when a person in that city is confirmed to have the disease. Each of these cities is linked to another city from which they contract the disease and to another city to which they transmit the infection. The resulting

city transmission network is denoted by $G = (V, C, E)$ where V is the set of nodes, $C \subset V$ is the set of central nodes, and E indicates the set of edges.

This construction results in a network with a tree-like structure. Each node is attributed with an infection date. The ensemble of epidemic trees rooted at each central node constitutes an epidemic forest. The resulting network is undirected; however, we use directed edges to emphasize the chronological flow of disease transmission. See Figure 1 for an example of a transmission network.
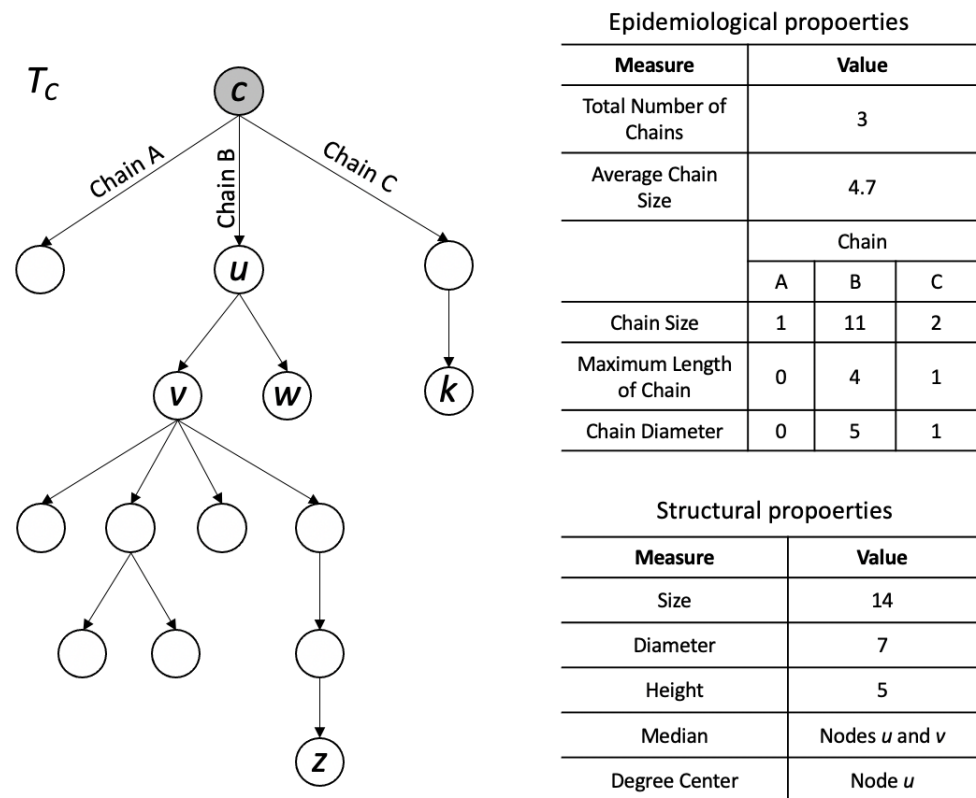

Epidemiological propoerties

Measure	Value		
Total Number of Chains	3		
Average Chain Size	4.7		
		Chain	
	A	B	C
Chain Size	1	11	2
Maximum Length of Chain	0	4	1
Chain Diameter	0	5	1

Structural propoerties

Measure	Value
Size	14
Diameter	7
Height	5
Median	Nodes u and v
Degree Center	Node u

Figure 1. An example of a transmission network. Tables list the epidemiological and structural properties of the epidemic tree rooted at node c with three transmission chains.

4.2. Transmission Network Analysis

Our goal is to use the topological properties of the transmission network to understand the role of cities and their connectivity in the disease propagation patterns. To do so, we analyze the developed network global properties such as node degree distribution and pair of node distances. Then, we analyze the epidemic tree rooted at each central node using two sets of measures: epidemiological and structural. Epidemiological measures are used to assess the evolving epidemiology of a disease. These metrics are crucial for understanding how infections propagate between nodes within the network, highlighting key transmission paths and the overall reach of the disease. Structural measures focus on the overall topology and connectivity of the epidemic network. These metrics are important for understanding the static properties of the network that might impact disease propagation. They provide insights into the network's connectivity and the hierarchical organization of infected nodes. Figure 1 shows an example of all properties.

In an epidemic tree, the root (source node) represents a source of infection. A transmission chain shows generations of infected nodes generated as a result of direct or indirect contact with the source node. Let T_c be the epidemic tree rooted at central node c, and $T_c = \{V, E\}$ be the set of epidemiological measures which include the following.

- **Total Number of Chains:** The Total Number of Chains indicates the number of chains starting at a central node [29]. The Total Number of Chains of a given central node c equals the number of node c's direct neighbors. It can be used to rank central nodes according to their role in direct disease spread. For example, in Figure 1, the Total Number of Chains of the shown epidemic tree is 3. This metric indicates the number of direct transmission paths originating from a central node, reflecting the node's direct impact on disease spread.

- **Chain Size:** The Chain Size indicates the number of nodes in each transmission chain excluding the central node [29]. The Chain Size of a given node v, where $v \in N(c)$ and c is a central node, equals the number of nodes in the Breadth First Search (BFS) tree rooted at v. It can be used to measure the influence of non-central nodes in spreading the disease. For example, the Chain Size of Chain B in Figure 1 is 11 since node u spreads the disease to 10 other nodes.

- **Maximum Length of Chains:** The Maximum Length of Chains shows the maximum number of directional edges in each chain [29]. The Maximum Length of Chains of a node v, where $v \in N(c)$ and c is a central node is equal to the height of the Breadth First Search (BFS) tree rooted at v. This metric captures the furthest extent a disease can travel within a chain. The Maximum Length of Chains of Chain B in Figure 1 is 4, showing the number of generations the disease traveled.

- **Average Chain Size:** The Average Chain Size represents the average number of cases resulting from an infection started at given central node [29]. It is computed by dividing the summation of Chain Sizes starting with same central node by the number of chains starting at a central node, providing an average measure of transmission spread. For example, the Average Chain Size of the epidemic tree in Figure 1 is 4.7 $((1 + 11 + 2)/3)$.

- **Chain Diameter:** The Chain Diameter measures the longest distance between any two nodes in a chain (excluding the central node), indicating the maximal spread within a chain. It can be obtained by computing the diameter of the undirected BFS tree rooted at node v, where $v \in N(c)$ and c is a central node. In Figure 1, the diameter of Chain B is five since the maximum distance connecting two nodes is five (path between nodes w and z).

The set of structural measures compares the hierarchical structures of each epidemic tree rooted at a central node. This set of measures includes:

- **Size:** The size of T_c indicates the total number of nodes that are infected as a result of a direct or indirect relationship with c, reflecting the infection's reach. It is computed as $|T_c| - 1$. The size measure provides a quantification of the infection ability of each central node. The size of the epidemic tree T_c in Figure 1 is 14.

- **Diameter:** The diameter of T_u represents the maximum path length between any two nodes in T_u. It is computed as $\max_{w,z \in V}\{d(w,z)\}$. The Diameter provides an estimation of the disease transmission distances. Note that the diameter does not take edge directions into account. In Figure 1, the diameter of T_c equals $d(k,z)$, which is seven.

- **Height:** The height of T_c shows the maximum number of directional edges in a path connecting c to a leaf node. It is computed as $\max_{v \in V}\{d(c,v)\}$. This measure is similar to the Maximum Length of Chains, except that it selects the maximum over all chains. In Figure 1, the height of the epidemic tree is five since $d(c,z) = 5$.

- **Median:** The median of T_c represents the vertex (or two connected vertices) closest to every other vertex in T_c (edge directions are not considered). It identifies disease spreader nodes with respect to node closeness to other nodes in the tree. The two nodes that represent the median of the epidemic tree in Figure 1 are nodes u and v.

- **Degree Center:** The Degree Center decides which node (or nodes) are most central with respect to their number of connections in an epidemic tree. It identifies disease spreader nodes with respect to node degrees. The central node according to degree in Figure 1 is node u.

- **Temporal Information:** A given epidemic tree can be temporally characterized by starting and ending dates [29]. The starting date of an epidemic tree T_c is equal to the infection date of its root node *c*, and its ending date is the last date on which a leaf node $v \in V$ was infected. The two dates define the disease spreading period [15].
- **Spatial Information:** A given epidemic tree can be spatially characterized by its geographic coverage [29], which describes the geographic area coverage by the tree [15].

5. Illustrative Example

We study the role and impact of city connectivity on COVID-19 disease spread in Saudi Arabia to demonstrate the proposed method.

5.1. Data

We utilize a COVID-19 dataset. The dataset is procured from the Saudi Ministry of Health [26], covering the period from 2 March 2020, to 25 April 2020, and consisting of 198,018 records. Each record within the dataset contains personal details, including age, gender, race, and city of residence. Additionally, the dataset encompasses information related to COVID-19 testing, such as the date of the test, the hospital where it was conducted, the test outcome, and the date the results were received. It also includes travel history, specifically noting whether individuals had visited any countries where the virus was endemic.

Two main data cleaning steps are applied to the dataset. First, we exclude any records that indicated a negative or not confirmed COVID-19 outcome, ensuring that our dataset focuses exclusively on confirmed cases. Second, records of individuals who tested positive for COVID-19 but had no travel history are excluded. This step ensures that the analysis concentrates on cities with initial imported cases. After applying these cleaning steps, the dataset is reduced to 1366 records.

After that, information from the individual records is extracted to build the COVID-19 city infection history file which includes the following sections (see Table A1 in Appendix A): city name, city region, date of first reported case (confirmation as a positive case), and date of first imported tested case (taking the swap). We include 119 main cities in Saudi Arabia. Not all cities appear in the obtained file. The reported dates for those cities are obtained from the daily dates provided by the online COVID-19 Dashboard: Saudi Arabia [57]. Table A1 shows that the date of the first imported tested case is much earlier compared to the date of the first reported case in 27 cities such as Arriad, Addammam, and Abha. This indicates that positive imported COVID-19 cases are actively spreading the disease for a period of time. This set of cities is considered to have a central role in disease transmission. The generated COVID-19 city infection history file and the constructed transmission network dataset are all available at https://github.com/halrashe/Covid19-Transmission-Network (accessed on 1 August 2024).

We assume that the potential infectious range of a city to cover the entire country since Saudi Arabia has well-developed road networks and transportation systems, and thus travel between any two cities is possible.

Our city transmission network, denoted by $G = (V, C, E)$ where V is the set of nodes, $C \subset V$ is the set of central nodes, and E is the set of edges, has a total of 119 nodes, 20 central nodes, and 118 edges (see Figure 2). The first positive COVID-19 case in Saudi Arabia was confirmed on 2 March 2020 in the city of Alqatif. Therefore, Alqatif city is selected to be the first infected node in the network. The remaining cities are added based on their first reported date (breaking ties arbitrarily). Let $I \subseteq V$ be a set of infected nodes, $S \subseteq V$ be a set of susceptible nodes, and $w \in I$ and $z \in S$ be two nodes (cities). A directed edge e_{wz} connects node *w* to node *z* if *w* is the closest in distance to node *z* than every other node $v \in I$. Because we focus on between-city analysis, nodes with an imported tested case after the date of 21 March 2020 (the date when all domestic transportation was suspended) are not considered central.
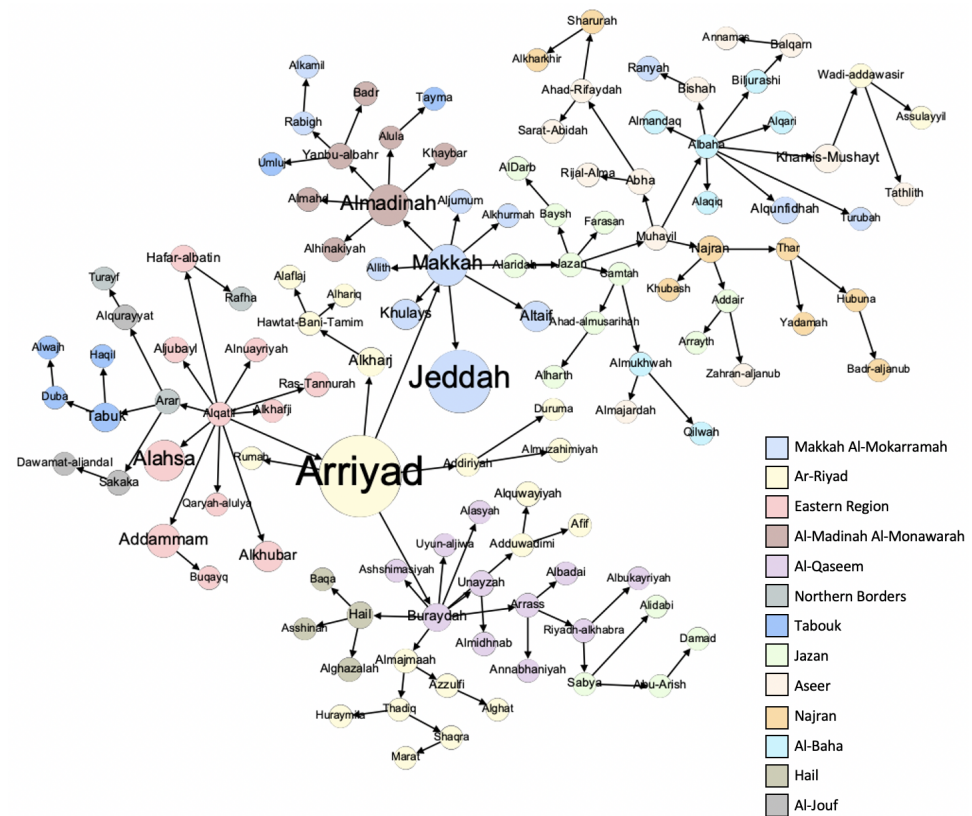
Figure 2. COVID-19 city transmission network between in Saudi Arabia. Nodes are partitioned according to their administrative regions. Node sizes are proportional to their populations.

5.2. Experimental Setup

Network construction and analyses were all conducted using the Python-based Networkx library [58]. Network visualizations were implemented using Gephi [59]. All experiments were run using a MacBook Pro, with the macOS Catalina operating system, version 10.15.4, and a 2 GHz Quad-Core Intel Core i5 with 16 GB RAM.

5.3. Results

Several cases test positive for COVID-19 after visiting infected countries in 27 Saudi cities, 20 of which occur before or on 21 March 2020 (the date when all domestic transportation was suspended). We consider all 20 cities as central nodes in the transmission network. Then, we measure several global, epidemiological, and structural properties of the transmission network and its chains. Tables 1 and 2 list several quantitative epidemiological and structural properties of COVID-19 transmission in Saudi Arabia.

5.3.1. Global Properties of Transmission Network

The network (epidemic forest) has 119 nodes and 118 edges (single connected component). The epidemic forest consists of 20 epidemic trees, each rooted at a central node. In total, 71% of edges connect cities that belong to the same administrative region. The maximum, minimum, and average outdegrees over all nodes are 11, 0, and 1, respectively. Figure 3 shows the degree distribution of all nodes. The degree distribution depicted in Figure 3 highlights a skewed pattern, with most nodes having a low outdegree and a few nodes exhibiting higher connectivity. This heterogeneity indicates that certain cities play disproportionately influential roles in disease transmission, acting as hubs in the network. Irrespective of edge directions, the average path length between nodes is three, and the network diameter is eight.

Table 1. Epidemiological properties of the transmission network chains for COVID-19 in Saudi Arabia.

	Central Node	Total Num of Chains	Avg Chain Size	Chain Size	Num of Chains	Max Length of Chains	Chain Diam
1	Alqatif	11	10.7	1	7	1	0
				2	2	2	1
				9	1	4	5
				98	1	8	13
2	Makkah almukarramah	8	7.4	1	6	1	0
				11	1	4	5
				42	1	6	8
3	Arriyad	5	19.4	1	1	1	0
				3	1	2	2
				4	1	3	2
				29	1	6	9
				60	1	7	10
4	Jazan	5	8.2	1	2	1	0
				2	1	2	1
				6	1	3	4
				31	1	5	8
5	Almadinah almunawwarah	5	2	1	3	1	0
				2	1	2	1
				5	1	4	4
6	Muhayil	3	10	6	1	4	4
				9	1	4	5
				15	1	4	6
7	Najran	3	2.7	1	1	1	0
				3	1	2	2
				4	1	3	3
8	Abha	2	2.5	1	1	1	0
				4	1	3	3
9	Adduwadimi	2	1	1	2	1	0
10	Alkharj	1	3	3	1	2	2
11	Addammam	1	1	1	1	1	0
12	Duba	1	1	1	1	1	0
13	Hafar-albatin	1	1	1	1	1	0
14	Aljubayl	0	0	0	0	0	0
15	Jeddah	0	0	0	0	0	0
16	Annamas	0	0	0	0	0	0
17	Alahsa	0	0	0	0	0	0
18	Altaif	0	0	0	0	0	0
19	Alkhubar	0	0	0	0	0	0
20	Alqunfidhah	0	0	0	0	0	0

5.3.2. Epidemiological Properties of Transmission Networks

Different epidemiological characteristics were captured by the quantitative measures of the transmission network: Total Number of Chains, Chain Size, Maximum Length of Chains, Average Chain Size, and Chain Diameter. The Total Number of Chains, Chain Size, and Average Chain Size describe the scope of COVID-19 transmission through one

source of infection (one central node). The Maximum Length of Chains and Chain Diameter describe the scale of COVID-19 transmission through one source of infection.

Table 2. Quantitative structural properties of transmission chains for COVID-19 in Saudi Arabia.

|	Central Node	Size	Diameter	Height	Median	Degree Center
1	Alqatif	118	13	8	Arriyad Makkah	Alqatif
2	Makkah	59	10	6	Jazan	Albaha
3	Arriyad	97	13	7	Arriyad Makkah	Albaha Makkah Buraydah
4	Jazan	41	8	5	Muhayil	Albaha
5	Almadinah	10	5	3	Almadinah Yanbu-albahr	Almadinah
6	Muhayil	30	8	4	Muhayil	Albaha
7	Najran	8	5	3	Najran Thar	Najran Thar Addair
8	Abha	5	4	3	Ahad-rifaydah	Ahad-rifaydah
9	Adduwadimi	2	2	1	Adduwadimi	Adduwadimi
10	Alkharj	3	2	2	Hawtat-bani-tamim	Hawtat-bani-tamim
11	Addammam	1	1	1	Addammam Buqayq	Addammam Buqayq
12	Duba	1	1	1	Duba Duba	Alwajh Alwajh
13	Hafar-albatin	1	1	1	Hafar-albatin Hafar-albatin	Rafha Rafha
14	Aljubayl	0	0	0	Aljubayl	Aljubayl
15	Jeddah	0	0	0	Jeddah	Jeddah
16	Annamas	0	0	0	Annamas	Annamas
17	Alahsa	0	0	0	Alahsa	Alahsa
18	Altaif	0	0	0	Altaif	Altaif
19	Alkhubar	0	0	0	Alkhubar	Alkhubar
20	Alqunfidhah	0	0	0	Alqunfidhah	Alqunfidhah
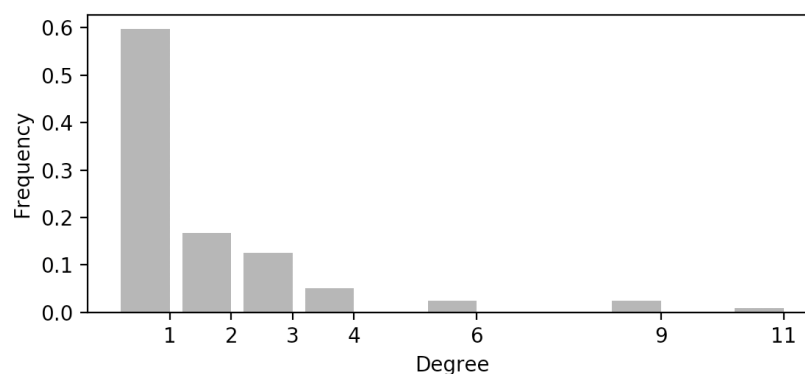
Figure 3. Degree distribution of the transmission network nodes.

According to Table 1, Alqatif city appears to have a bigger role in the spread of COVID-19 (Total Number of Chains is 11). This can be due to the fact that Alqatif was the first city to host a positive COVID-19 case in Saudi Arabia. This can also be due to Alqatif's geographic location (or a combination of both). The Maximum Length of a Transmission

Chain in Alqatif reaches 8, which suggests that the spread of COVID-19 in Saudi Arabia was highly affected by in-between city transmission. The Average Chain Size is 10.7 (the smallest Chain Size is one and the largest is 98). This suggests that COVID-19 may have traveled to 10 cities (depth-wise) before it was controlled.

Table 1 also shows that Makkah, the holiest city, was a vital source of the disease's transmission. A total of eight transmission chains originated from Makkah with a Maximum Length of 6 and a Chain Size of 42. Each of Arriyad, Jazan, and Almadinah generated a total of five transmission chains with average sizes of 19.4, 8.2, and 2, respectively. The Maximum Length of Chains is 7 in Arriyad, 5 in Jazan, and 4 in Almadinah.

Several central cities generated fewer transmission chains including Muhayil, Najran, Abha, and Adduwadimi (Total Number of Chains is between two and three). Interestingly, the produced transmission chains are not necessarily shorter (compared with the Average Chain Size of central cities that produced more chains). For example, Muhayil's Average Chain Size is larger than Makkah's Average Chain Size, although Makkah produced eight chains and Muhayil produced three chains.

Some cities appear to have more negligible transmission effects during the disease transmission period. For example, Addamam, Duba, and Hafar-albatin caused a transmission to only a single city. Aljubayl, Jeddah, Annamas, Alahsa, Altaif, Alkhubar, and Alqunfidhah did not produce any disease transmissions across the network.

Figure 4 show two epidemic trees rooted at central nodes Jazan (T_{Jazan}) and Almadinah ($T_{Almadinah}$), respectively. The different nodes are colored according to the administrative regions they belong to. The figure shows that both central nodes have caused disease transmission within and outside of their administrative regions (Jazan spread the disease to five other regions and Almadinah to two other regions). Both trees have the same Total Number of Chains. However, the Average Chain Size of T_{Jazan} is larger than that of $T_{Almadinah}$.
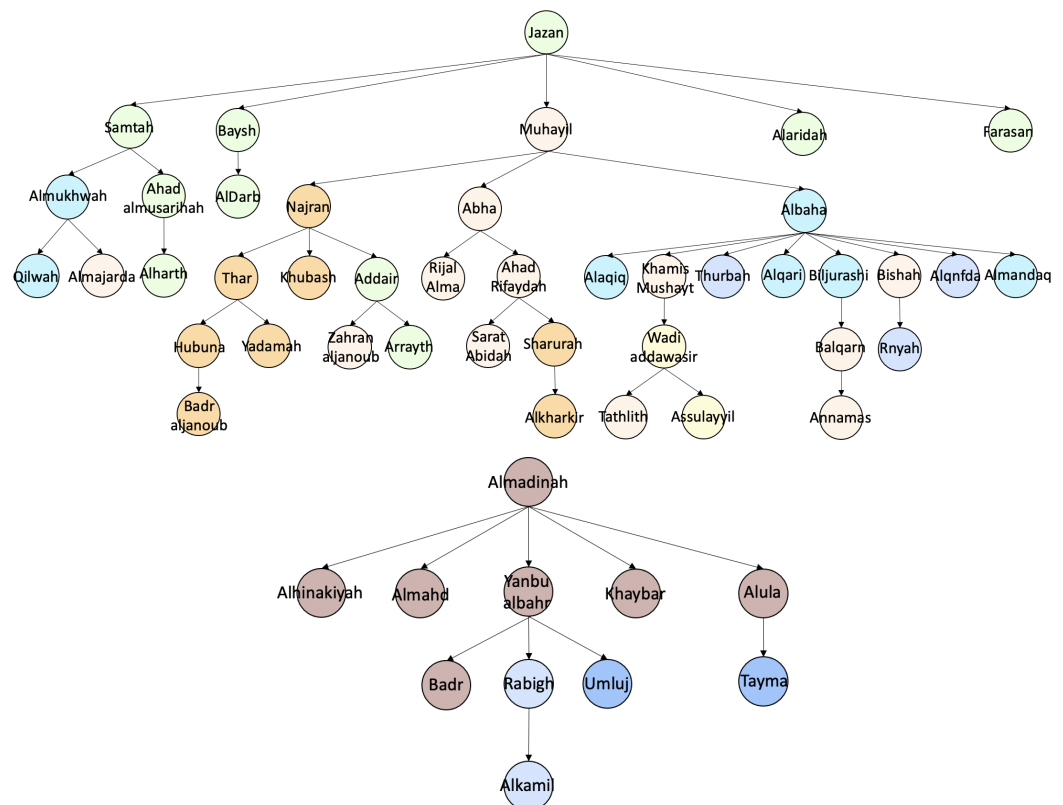

Figure 4. The epidemic trees rooted at two central nodes: Jazan (**top**) and Almadinah (**bottom**).

5.3.3. Structural Properties of Transmission Networks

The second set of measures examines the structural properties of the epidemic trees rooted at each central node. Those measures provide insights about the between-city transmission events. Seven measures were considered for each epidemic tree: Size, Diameter, Height, Median, Degree Center, and Temporal and Spatial Information. The Size property indicates the total number of infections arising from each infected central node. Table 2 shows that the epidemic trees rooted at Alqatif, Arriyad, and Makkah resulted in larger infection sizes compared to the other epidemic trees. The three trees also have the largest diameters and heights, indicating their significant role in the disease spread. The Diameters of each of $T_{Alqatif}$, T_{Makkah}, and $T_{Arriyad}$ are 13, 10, and 13, respectively. The Heights of $T_{Alqatif}$, T_{Makkah}, and $T_{Arriyad}$ are 8, 6, and 7, respectively.

Additionally, Jazan generated a total of 41 infections with a Diameter of eight and a Height of five. Muhayil produced a total of 30 infections. The Diameter and Height of $T_{Muhayil}$ are 8 and 4, respectively. Almadinah and Najran (with sizes of 10 and 8, respectively) both have a Diameter of 5 and Height of 3. Abha, Alkharj, and Adduwadimi generated 5, 3, and 2 total infections. The Diameters are 4, 2, and 2, and the Heights are 3, 2, and 1, respectively.

Node centrality measures identify superspreader nodes in each tree. We use two centrality measures: Median (node or nodes closest to every other node with respect to distance) and Degree Center (node or nodes with the largest number of connections). Interestingly, the central node and the median are represented by different nodes in most epidemic trees. For example, the Median in $T_{Alqatif}$ is represented by two nodes: Arriyad and Makkah. The Median in T_{Makkah} is represented by one node: Jazan. Similarly, in most epidemic trees, the central node and the Degree Center are not necessarily equal. For example, the Degree Center in both T_{Makkah} and T_{Jazan} is Albaha (see Figure 4. In fact, Albaha appears to represent the Degree Center in several epidemic trees including T_{Makkah}, $T_{Arriyad}$, and $T_{Muhayil}$.

Figure 5 and Table 3 show the temporal and spatial information of several epidemic trees. Multiple epidemic trees have overlapping temporal information and geographic coverages. For example, $T_{Muhayil}$ is a subset of T_{Jazan}.

Table 3. Temporal and spatial information of 13 epidemic trees.

	Central Node	Starting Date	Ending Date	Coverage (km^2)
1	Alqatif	2 March 2020	23 June 2020	1,862,582
2	Arriyad	9 March 2020	23 June 2020	1,066,118
3	Makkah	10 March 2020	22 June 2020	642,964
4	Jazan	16 March 2020	22 June 2020	351,874
5	Muhayil	19 March 2020	22 June 2020	339,969
6	Almadinah	20 March 2020	23 June 2020	206,758
7	Najran	23 March 2020	11 June 2020	65,481
8	Abha	24 March 2020	22 June 2020	88,921
9	Adduwadmi	30 March 2020	26 April 2020	79,475
10	Alkharj	9 April 2020	23 May 2020	81,057
11	Addammam	15 March 2020	24 April 2020	7778
12	Duba	3 April 2020	6 April 2020	23,046
13	Hafar-albatin	20 March 2020	24 April 2020	87,496

5.3.4. Validation

Our goal is to validate our city transmission network generation. Our proposed network generation model uses geographic distance between cities as the single factor that affect the infection process (the infection always progresses to a susceptible city from the closest infected one). To validate the generated network, we need to decide the factor or factors that most affect disease transmission between cities, for example, mobility and population.
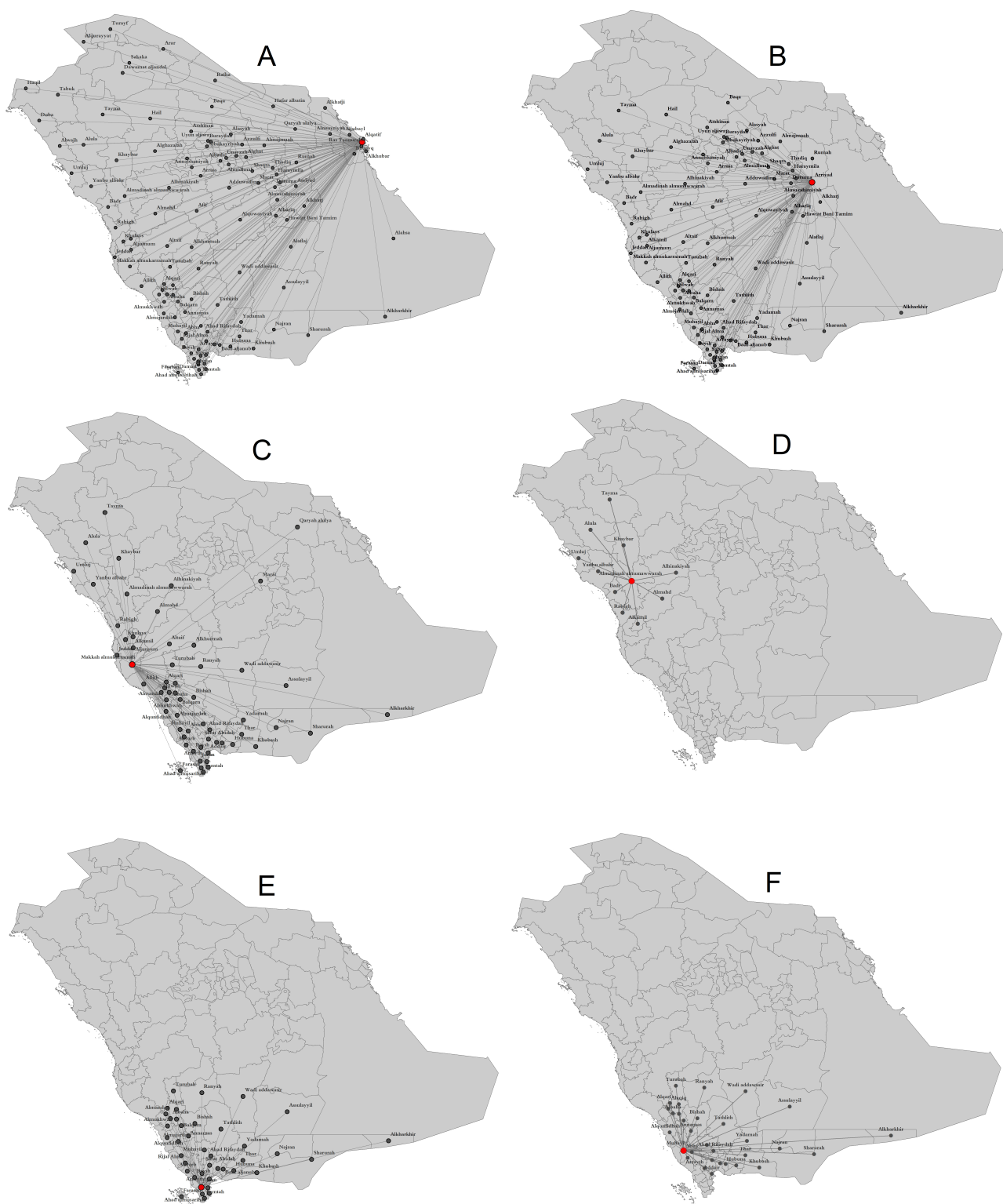
Figure 5. Geographic coverages of six epidemic trees: (**A**) $T_{Alqatif}$, (**B**) $T_{Arriyad}$, (**C**) T_{Makkah}, (**D**) $T_{Almadinah}$, (**E**) T_{Jazan}, and (**F**) $T_{Muhayil}$. The red dots indicate the root cities of the respective epidemic trees.

We analyze the relationship between city populations and the order by which each city was infected. We use Pearson's product–moment correlation to find the correlation between the population and the order (see Figure 6). The analysis indicates a moderate

negative relationship ($r = -0.39$), suggesting that nodes with higher populations are more likely to become infected earlier than lower population nodes.

Based on this result, we create another transmission model that takes destination city population into account. Given an infected node u and a non-infected node v, the spread of infection from u to v occurs with a probability p_{uv} proportional to the population of node v (resembling city mobility) as follows $p_{uv} = \alpha * (population_u / population_{sum})$, where α is a constant and $population_{sum}$ is the population sum over all cities.

We use this model to create several transmission network ensembles, each of which simulates a disease transmission incident. The first infected node is set to Alqatif, and α is set to 0.1. For each network, we count the Size (number of infected nodes in the tree rooted at a central node) of each central node and compare them with the tree sizes of the original transmission network. Figure 7 compares the epidemic tree sizes of the original network and the average of 100 simulated networks using the model described above. The Pearson correlation coefficient between the two curves is 0.78, indicating a positive relationship. This implies that no matter what the infection order is, a city population plays a big role in its infectivity.
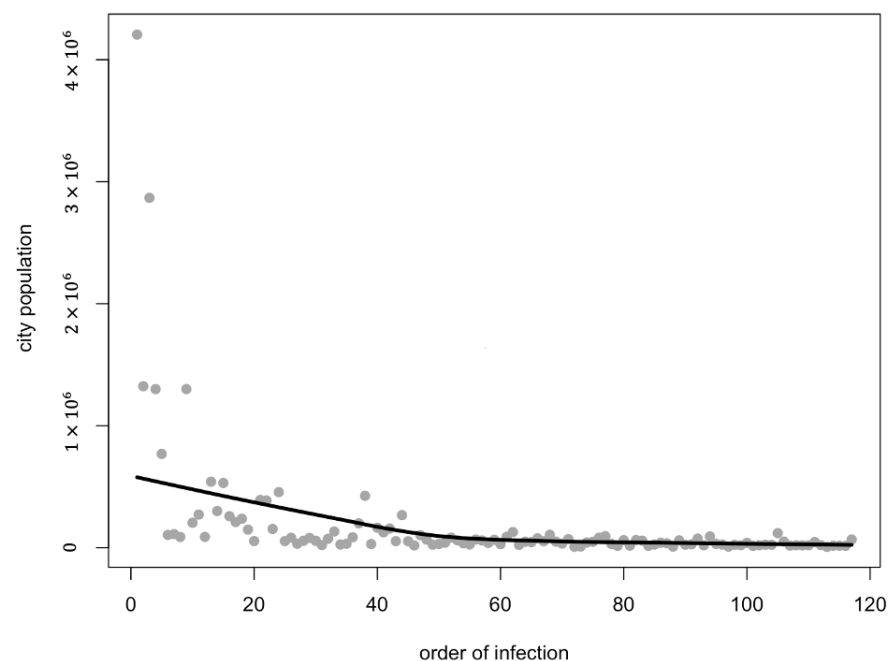

Figure 6. The correlation between city populations and the order in which cities were infected.
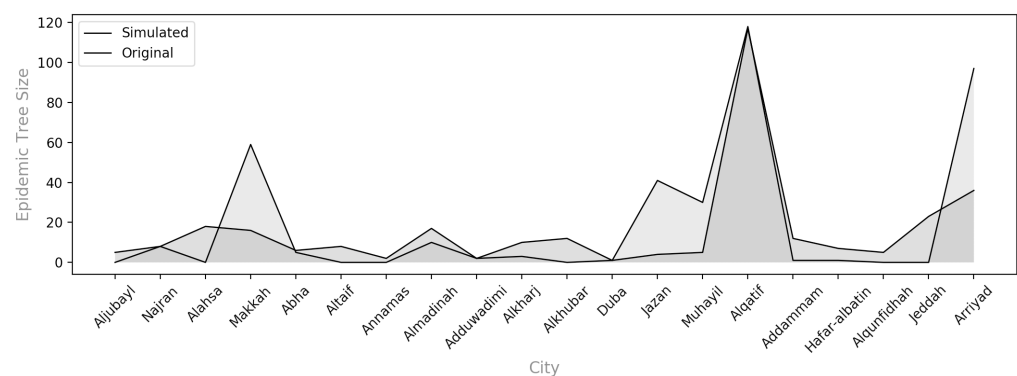

Figure 7. Comparing tree sizes of original and simulated transmission networks.

5.4. Discussion

Understanding the behavior and the spread patterns of a disease helps to effectively and cost-efficiently contain it. Tracing the transmission chains across the cities is one of the crucial tools for managing the pandemic. It can assist authorities in tailoring their efforts and setting the appropriate control measures, focusing on superspreader cities instead of overall lockdowns, to alleviate the otherwise devastating effects on economies.

Considering the importance of between-city movement in disease transmission, we propose constructing a city transmission network that models the spread of a disease. Network-based approaches provide additional insights into disease spread dynamics that are not captured by alternative methods. Unlike traditional models, network-based approaches can incorporate more information and handle complex interactions between geographical locations. This level of information richness offers a better representation of disease transmission through specific pathways and superspreader cities. The network-based method improves epidemic forecasting accuracy while also providing actionable information for more effective disease control and prevention strategies.

Our network is built based on epidemiological data about the disease and geographic distances between cities. Then, quantitative analysis is used to compare the impact of different cities on the disease transmission process. We focus on epidemiological and structural effects of each source of infection, including tracing the infection and discovering superspreader cities.

Identifying the source (or sources) of an infection is important; however, deciding superspreader cities (with the highest potential to spread an infection) is vital for disease prevention. In our example, Alqatif was the first city with a positive COVID-19 case in Saudi Arabia. However, tracing the transmission chains in the city transmission network revealed that the median (center) of this tree was Arriyad and Makkah. This indicates that the role played by Arriyad and Makkah cities during disease transmission was bigger compared to that of Alqatif. Consequently, authorities should prioritize enforcing lockdowns in these cities to effectively mitigate the spread of disease. By focusing the preventative measures and resources in Arriyad and Makkah, where the transmission dynamics have demonstrated a central role in the network, targeted interventions can be more strategically implemented. This approach not only curtails the further spread of the virus from these hubs but also allows for a more efficient allocation of healthcare resources and public health responses, potentially leading to a quicker containment of outbreaks.

Our analysis also shows that a city infection impact is not always local. In most cases, the impact crosses the regional borders of a city to other cities in different regions. For example, Makkah city spread the disease to other cities within its region (Altaif, Alqunfidhah, and Khulays) and others in Almadinah, Jazan, and Albaha regions. This type of analysis can help decision makers with disease prevention and control strategies, for example, determining priorities and narrowing the scope of quarantine.

Because the model relies on the daily number of confirmed cases, it enables the real-time identification of critical locations for early intervention with a certain degree of precision. It uses epidemiological metrics, such as the Total Number of Chains at each central node, to decide the role of these nodes in disease spread, even before the pandemic ends and without complete time series data. This capability for early detection could have allowed authorities to implement targeted quarantine measures to effectively mitigate the impact of an outbreak. Furthermore, our model facilitates the efficient allocation and management of healthcare resources, thereby reducing the pressures on national healthcare systems. It empowers authorities to more effectively distribute medical supplies and other essential items to strategically important cities. By preparing essential nodes in the virus propagation network ahead of time, we can ensure better readiness for potential outbreaks.

6. Conclusions

In order to better control a running disease, it is important to understand how it propagates. Individuals and the disease transmission between them or (groups of them) can be represented as a network. Such a network can be constructed to provide important information on the epidemiological dynamics. Looking into the network structure and possible disease transmission paths may help with disease management and control. Here, we proposed building a city transmission network to simulate the spread of a disease. The constructed network supports comparing the impact of cities on disease transmission using quantitative methods.

For each source of infection, we investigated the epidemiological and structural impacts, as well as superspreaders. Our analysis suggests that identifying superspreader cities is crucial in the early stages of an epidemic, more so than community-level disease transmission. This is because the effects of infections in these cities are not confined to local boundaries but can extend across regional borders, impacting neighboring areas. We show the example of COVID-19 in Saudi Arabia. In this example, there is evidence that Arriyad and Makkah played a larger influence in the spread of disease than the city of Alqatif.

The proposed method for investigating superspreading events and disease transmission dynamics can be applied in different regions by considering region-specific factors, human mobility patterns, and transmission dynamics. The methodology's adaptability and effectiveness in estimating superspreading environments make it a valuable tool for studying disease transmission dynamics across various geographical settings. Moreover, the model can be applied in real time to offer insights into the role of cities in disease transmission.

The proposed method has a few challenges and limitations. First, the available epidemiological data of each infected individual usually lack complete contact history. The exact exposure history (including domestic travel history) of each individual is important for accurate network construction. Second, while it is often straightforward to identify individuals' international travel history, tracking their domestic travel can be more challenging. Third, the between-city distance was the only criterion used to decide disease transmission from one city to another. A probabilistic model that considers other criteria (human mobility, city population, etc.) would have provided more realistic results.

Data Availability Statement: The history file and the constructed transmission network dataset and analysis code are all available at https://github.com/halrashe/Covid19-Transmission-Network (accessed on 1 August 2024).

Conflicts of Interest: The authors declare no conflicts of interest.

Appendix A

Table A1. COVID-19 city infection history file with the following sections: cities, their regions, date and frequency of first reported case, and first tested case in each city, respectively.

	City	Region	Reported Date	Freq	Tested Date	Freq
1	Alahsa	Eastern Region	14 March 2020	1	11 March 2020	2
2	Alaflaj	Ar-Riyad	6 May 2020	1		
3	Alasyah	Al-Qaseem	23 May 2020	1		
4	Albaha	Al-Baha	20 March 2020	1	20 March 2020	1
5	Albadai	Al-Qaseem	31 March 2020	1		
6	Albukayriyah	Al-Qaseem	18 April 2020	1		
7	Alhariq	Ar-Riyad	23 May 2020	1		
8	Addiriyah	Ar-Riyad	4 April 2020	1		
9	Addammam	Eastern Region	15 March 2020	1	3 March 2020	1
10	Adduwadimi	Ar-Riyad	30 March 2020	1	28 March 2020	1
11	Alaridah	Jazan	26 April 2020	14		
12	Alaqiq	Al-Baha	23 April 2020	1		
13	Alghat	Ar-Riyad	22 June 2020	2		
14	Alghazalah	Hail	6 May 2020	1		
15	Abha	Aseer	24 March 2020	6	19 March 2020	2
16	Abu Arish	Jazan	26 April 2020	10		
17	Ahad almusarihah	Jazan	26 May 2020	1		
18	Ahad Rifaydah	Aseer	2 April 2020	1		
19	Afif	Ar-Riyad	26 April 2020	2		
20	Addair	Jazan	7 May 2020	1		
21	Alharth	Jazan	1 June 2020	1		
22	Alhinakiyah	Al-Madinah Al-Monawarah	1 April 2020	1		
23	Alidabi	Jazan	4 May 2020	1		
24	Aljubayl	Eastern Region	25 March 2020	1	21 March 2020	1
25	Aljumum	Makkah Al-Mokarramah	21 May 2020	3		
26	Alkamil	Makkah Al-Mokarramah	6 May 2020	1		
27	Alkhafji	Eastern Region	26 March 2020	1		
28	Alkharj	Ar-Riyad	9 April 2020	2	6 April 2020	1
29	Alkharkhir	Najran	22 June 2020	4		
30	Alkhubar	Eastern Region	22 March 2020	4	11 March 2020	1
31	Alkhurmah	Makkah Al-Mokarramah	23 April 2020	1		
32	Allith	Makkah Al-Mokarramah	16 April 2020	2		

Table A1. *Cont.*

	City	Region	Reported Date	Freq	Tested Date	Freq
33	Almadinah almunawwarah	Al-Madinah Al-Monawarah	20 March 2020	1	19 March 2020	2
34	Almahd	Al-Madinah Al-Monawarah	24 April 2020	3		
35	Almajardah	Aseer	26 April 2020	1		
36	Almajmaah	Ar-Riyad	4 April 2020	1		
37	Almandaq	Al-Baha	23 April 2020	1		
38	Almidhnab	Al-Qaseem	22 April 2020	1		
39	Almukhwah	Al-Baha	21 April 2020	3		
40	Almuzahimiyah	Ar-Riyad	24 April 2020	1		
41	Alnuayriyah	Eastern Region	21 March 2020	1		
42	Alqari	Al-Baha	21 May 2020	1		
43	Alqatif	Eastern Region	2 March 2020	1	19 March 2020	1
44	AlDarb	Jazan	2 May 2020	1		
45	Alqunfidhah	Makkah Al-Mokarramah	23 March 2020	1	20 March 2020	1
46	Alqurayyat	Al-Jouf	16 April 2020	2		
47	Alquwayiyah	Ar-Riyad	10 April 2020	2		
48	Altaif	Makkah Al-Mokarramah	23 March 2020	6	19 March 2020	1
49	Alula	Al-Madinah Al-Monawarah	7 April 2020	1		
50	Alwajh	Tabouk	6 April 2020	1		
51	Annabhaniyah	Al-Qaseem	11 June 2020	1		
52	Annamas	Aseer	22 May 2020	1	19 March 2020	2
53	Arar	Northern Borders	25 March 2020	2	22 March 2020	2
54	Arrass	Al-Qaseem	30 March 2020	1	26 March 2020	1
55	Arrayth	Jazan	10 June 2020	1		
56	Arriyad	Ar-Riyad	9 March 2020	1	7 March 2020	1
57	Ashshimasiyah	Al-Qaseem	22 June 2020	11		
58	Asshinan	Hail	20 June 2020	1		
59	Assulayyil	Ar-Riyad	13 May 2020	1		
60	Azzulfi	Ar-Riyad	15 April 2020	1		
61	Badr	Al-Madinah Al-Monawarah	23 June 2020	1		
62	Badr aljanub	Najran	11 June 2020	1		
63	Balqarn	Aseer	17 May 2020	7		
64	Baqa	Hail	22 May 2020	1		
65	Baysh	Jazan	19 April 2020	1		
66	Biljurashi	Al-Baha	24 April 2020	1		

Table A1. *Cont.*

	City	Region	Reported Date	Freq	Tested Date	Freq
67	Bishah	Aseer	20 March 2020	1		
68	Buqayq	Eastern Region	24 April 2020	3		
69	Buraydah	Al-Qaseem	26 March 2020	1	22 March 2020	1
70	Damad	Jazan	27 May 2020	1		
71	Dawamat aljandal	Al-Jouf	27 April 2020	1		
72	Duba	Tabouk	3 April 2020	1	18 March 2020	1
73	Duruma	Ar-Riyad	4 May 2020	1		
74	Farasan	Jazan	10 June 2020	2		
75	Hafar albatin	Eastern Region	20 March 2020	1	18 March 2020	1
76	Hail	Hail	14 April 2020	1	12 April 2020	1
77	Haqil	Tabouk	16 May 2020	1		
78	Hawtat Bani Tamim	Ar-Riyad	4 May 2020	1		
79	Hubuna	Najran	3 June 2020	1		
80	Huraymila	Ar-Riyad	12 May 2020	1		
81	Jazan	Jazan	16 March 2020	1	14 March 2020	1
82	Jeddah	Makkah Al-Mokarramah	11 March 2020	1	8 March 2020	2
83	Khamis Mushayt	Aseer	28 March 2020	3		
84	Khaybar	Al-Madinah Al-Monawarah	4 May 2020	1		
85	Khubash	Najran	22 May 2020	1		
86	Khulays	Makkah Al-Mokarramah	10 April 2020	1		
87	Makkah almukarramah	Makkah Al-Mokarramah	10 March 2020	1	9 March 2020	4
88	Marat	Ar-Riyad	15 May 2020	1		
89	Muhayil	Aseer	19 March 2020	1	17 March 2020	1
90	Najran	Najran	23 March 2020	1	18 March 2020	1
91	Qaryah alulya	Eastern Region	20 May 2020	1		
92	Qilwah	Al-Baha	11 May 2020	1		
93	Rabigh	Makkah Al-Mokarramah	19 April 2020	2		
94	Rafha	Northern Borders	24 April 2020	1		
95	Ranyah	Makkah Al-Mokarramah	28 May 2020	1		
96	Ras Tannurah	Eastern Region	29 March 2020	1		
97	Rijal Alma	Aseer	16 April 2020	3		
98	Riyadh alkhabra	Al-Qaseem	9 April 2020	1	6 April 2020	1
99	Rumah	Ar-Riyad	16 May 2020	1		

Table A1. *Cont.*

	City	Region	Reported Date	Freq	Tested Date	Freq
100	Sabya	Jazan	12 April 2020	2		
101	Sakaka	Al-Jouf	24 April 2020	5		
102	Samtah	Jazan	30 March 2020	1		
103	Sarat Abidah	Aseer	9 May 2020	1		
104	Shaqra	Ar-Riyad	12 May 2020	1		
105	Sharurah	Najran	7 April 2020	4		
106	Tabuk	Tabouk	29 March 2020	1	1 April 2020	2
107	Tathlith	Aseer	8 May 2020	1		
108	Tayma	Tabouk	15 May 2020	1		
109	Thadiq	Ar-Riyad	8 May 2020	1		
110	Thar	Najran	25 May 2020	6		
111	Turayf	Northern Borders	12 May 2020	18		
112	Turubah	Makkah Al-Mokarramah	25 April 2020	1		
113	Umluj	Tabouk	30 April 2020	1		
114	Unayzah	Al-Qaseem	9 April 2020	2		
115	Uyun aljiwa	Al-Qaseem	21 May 2020	5		
116	Wadi addawasir	Ar-Riyad	26 April 2020	2		
117	Yadamah	Najran	1 June 2020	1		
118	Yanbu albahr	Al-Madinah Al-Monawarah	8 April 2020	1		
119	Zahran aljanub	Aseer	21 May 2020	2		

References

1. Eames, K.T.D.; Read, J.M. Networks in Epidemiology. In Proceedings of the Bio-Inspired Computing and Communication, Berlin/Heidelberg, Germany, 2–5 April 2008; Lecture Notes in Computer Science; pp. 79–90.
2. Sun, K.; Wang, W.; Gao, L.; Wang, Y.; Luo, K.; Ren, L.; Zhan, Z.; Chen, X.; Zhao, S.; Huang, Y.; et al. Transmission heterogeneities, kinetics, and controllability of SARS-CoV-2. *Science* **2021**, *371*, eabe2424. [CrossRef]
3. Van Gunten, T. Visualizing the Network Structure of COVID-19 in Singapore. *Socius* **2021**, *7*, 23780231211000171. [CrossRef] [PubMed]
4. Russell, T.W.; Wu, J.T.; Clifford, S.; Edmunds, W.J.; Kucharski, A.J.; Jit, M. Effect of internationally imported cases on internal spread of COVID-19: A mathematical modelling study. *Lancet Public Health* **2021**, *6*, e12–e20. [CrossRef] [PubMed]
5. Godin, A.; Xia, Y.; Buckeridge, D.L.; Mishra, S.; Douwes-Schultz, D.; Shen, Y.; Lavigne, M.; Drolet, M.; Schmidt, A.M.; Brisson, M.; et al. The role of case importation in explaining differences in early SARS-CoV-2 transmission dynamics in Canada—A mathematical modeling study of surveillance data. *Int. J. Infect. Dis.* **2021**, *102*. [CrossRef] [PubMed]
6. Lewis, D. Superspreading drives the COVID pandemic–and could help to tame it. *Nature* **2021**, *590*, 544–547. [CrossRef] [PubMed]
7. Oka, T.; Wei, W.; Zhu, D. The effect of human mobility restrictions on the COVID-19 transmission network in China. *PLoS ONE* **2021**, *16*, e0254403. [CrossRef]
8. Benvenuto, D.; Giovanetti, M.; Vassallo, L.; Angeletti, S.; Ciccozzi, M. Application of the ARIMA model on the COVID-2019 epidemic dataset. *Data Brief* **2020**, *29*, 105340. [CrossRef]
9. Biala, T.A.; Afolabi, Y.O.; Khaliq, A.Q.M. How efficient is contact tracing in mitigating the spread of COVID-19? A mathematical modeling approach. *Appl. Math. Model.* **2022**, *103*, 714–730. [CrossRef]
10. Yang, Z.; Zeng, Z.; Wang, K.; Wong, S.S.; Liang, W.; Zanin, M.; Liu, P.; Cao, X.; Gao, Z.; Mai, Z.; et al. Modified SEIR and AI prediction of the epidemics trend of COVID-19 in China under public health interventions. *J. Thorac. Dis.* **2020**, *12*, 165. [CrossRef]

11. Lin, Q.; Zhao, S.; Gao, D.; Lou, Y.; Yang, S.; Musa, S.S.; Wang, M.H.; Cai, Y.; Wang, W.; Yang, L.; et al. A conceptual model for the coronavirus disease 2019 (COVID-19) outbreak in Wuhan, China with individual reaction and governmental action. *Int. J. Infect. Dis.* **2020**, *93*, 211–216. [CrossRef]

12. Liu, F.; Li, X.; Zhu, G. Using the contact network model and Metropolis-Hastings sampling to reconstruct the COVID-19 spread on the "Diamond Princess". *Sci. Bull.* **2020**, *65*, 1297–1305. [CrossRef] [PubMed]

13. Alrasheed, H.; Althnian, A.; Kurdi, H.; Al-Mgren, H.; Alharbi, S. COVID-19 Spread in Saudi Arabia: Modeling, Simulation and Analysis. *Int. J. Environ. Res. Public Health* **2020**, *17*, 7744. [CrossRef] [PubMed]

14. Peirlinck, M.; Linka, K.; Costabal, F.S.; Kuhl, E. Outbreak dynamics of COVID-19 in China and the United States. *Biomech. Model. Mechanobiol.* **2020**, *19*, 2179–2193. [CrossRef] [PubMed]

15. Li, M.; Shi, X.; Li, X.; Ma, W.; He, J.; Liu, T. Epidemic forest: A spatiotemporal model for communicable diseases. *Ann. Am. Assoc. Geogr.* **2019**, *109*, 812–836. [CrossRef]

16. Gürsakal, N.; Batmaz, B.; Aktuna, G. Drawing transmission graphs for COVID-19 in the perspective of network science. *Epidemiol. Infect.* **2020**, *148*, e269. [CrossRef] [PubMed]

17. Hâncean, M.G.; Perc, M.; Lerner, J. Early spread of COVID-19 in Romania: Imported cases from Italy and human-to-human transmission networks. *R. Soc. Open Sci.* **2020**, *7*, 200780. [CrossRef] [PubMed]

18. Wong, N.S.; Lee, S.S.; Kwan, T.H.; Yeoh, E.K. Settings of virus exposure and their implications in the propagation of transmission networks in a COVID-19 outbreak. *Lancet Reg. Health West. Pac.* **2020**, *4*, 100052. [CrossRef] [PubMed]

19. Kırbıyık, U. Network Characteristics and Visualization of COVID-19 Outbreak in a Large Detention Facility in the United States—Cook County, Illinois, 2020. *MMWR Morb. Mortal. Wkly. Rep.* **2020**, *69*, 1625–1630 .

20. Changruenngam, S.; Bicout, D.J.; Modchang, C. How the individual human mobility spatio-temporally shapes the disease transmission dynamics. *Sci. Rep.* **2020**, *10*, 11325. [CrossRef]

21. Maheshwari, P.; Albert, R. Network model and analysis of the spread of COVID-19 with social distancing. *Appl. Netw. Sci.* **2020**, *5*, 100. [CrossRef]

22. Klise, K.; Beyeler, W.; Finley, P.; Makvandi, M. Analysis of mobility data to build contact networks for COVID-19. *PLoS ONE* **2021**, *16*, e0249726. [CrossRef] [PubMed]

23. Loeffler-Wirth, H.; Schmidt, M.; Binder, H. Covid-19 transmission trajectories–monitoring the pandemic in the worldwide context. *Viruses* **2020**, *12*, 777. [CrossRef] [PubMed]

24. Cardoso, B.H.F.; Gonçalves, S. Universal scaling law for human-to-human transmission diseases. *Europhys. Lett.* **2021**, *133*, 58001. [CrossRef]

25. Hu, H.; Nigmatulina, K.; Eckhoff, P. The scaling of contact rates with population density for the infectious disease models. *Math. Biosci.* **2013**, *244*, 125–134. [CrossRef] [PubMed]

26. Ministry of Health Saudi Arabia. Ministry of Health Saudi Arabia. 2022. Available online: https://www.moh.gov.sa/en/Pages/Default.aspx (accessed on 1 August 2024).

27. Newman, M.E.; Strogatz, S.H.; Watts, D.J. Random graphs with arbitrary degree distributions and their applications. *Phys. Rev. E* **2001**, *64*, 026118. [CrossRef] [PubMed]

28. Kiss, I.Z.; Green, D.M.; Kao, R.R. The network of sheep movements within Great Britain: Network properties and their implications for infectious disease spread. *J. R. Soc. Interface* **2006**, *3*, 669–677. [CrossRef] [PubMed]

29. Luo, C.; Ma, Y.; Jiang, P.; Zhang, T.; Yin, F. The construction and visualization of the transmission networks for COVID-19: A potential solution for contact tracing and assessments of epidemics. *Sci. Rep.* **2021**, *11*, 8605. [CrossRef] [PubMed]

30. Williamson, S.G. *Combinatorics for Computer Science*; Courier Corporation: North Chelmsford, MA, USA, 2002.

31. Mesbahi, M.; Egerstedt, M. *Graph Theoretic Methods in Multiagent Networks*; Princeton University Press: Princeton, NJ, USA, 2010.

32. Kansky, K.; Danscoine, P. Measures of network structure. *FLUX Cah. Sci. Int. RÉSeaux Territ.* **1989**, *5*, 89–121. [CrossRef]

33. Haydon, D.T.; Chase-Topping, M.; Shaw, D.; Matthews, L.; Friar, J.; Wilesmith, J.; Woolhouse, M. The construction and analysis of epidemic trees with reference to the 2001 UK foot–and–mouth outbreak. *Proc. R. Soc. Lond. Ser. Biol. Sci.* **2003**, *270*, 121–127. [CrossRef]

34. Napp, S.; Allepuz, A.; Purse, B.; Casal, J.; García-Bocanegra, I.; Burgin, L.; Searle, K. Understanding spatio-temporal variability in the reproduction ratio of the bluetongue (BTV-1) epidemic in Southern Spain (Andalusia) in 2007 using epidemic trees. *PLoS ONE* **2016**, *11*, e0151151. [CrossRef]

35. Lau, M.S.; Dalziel, B.D.; Funk, S.; McClelland, A.; Tiffany, A.; Riley, S.; Metcalf, C.J.E.; Grenfell, B.T. Spatial and temporal dynamics of superspreading events in the 2014–2015 West Africa Ebola epidemic. *Proc. Natl. Acad. Sci. USA* **2017**, *114*, 2337–2342. [CrossRef] [PubMed]

36. Diekmann, O.; Heesterbeek, J.A.P. *Mathematical Epidemiology of Infectious Diseases: Model Building, Analysis and Interpretation*; John Wiley & Sons: Hoboken, NJ, USA, 2000; Volume 5.

37. Kao, R.R.; Danon, L.; Green, D.M.; Kiss, I.Z. Demographic structure and pathogen dynamics on the network of livestock movements in Great Britain. *Proc. R. Soc. Biol. Sci.* **2006**, *273*, 1999–2007. [CrossRef] [PubMed]

38. John, R.S.; Miller, J.C.; Muylaert, R.L.; Hayman, D.T. High connectivity and human movement limits the impact of travel time on infectious disease transmission. *J. R. Soc. Interface* **2024**, *21*, 20230425. [CrossRef] [PubMed]

39. Guo, Z.; Li, J.; Xiao, G.; Gong, L.; Wang, Y. Dynamic model of respiratory infectious disease transmission by population mobility based on city network. *R. Soc. Open Sci.* **2022**, *9*, 221232. [CrossRef] [PubMed]

40. Leung, W.T.; Rudge, J.W.; Fournié, G. Simulating contact networks for livestock disease epidemiology: A systematic review. *J. R. Soc. Interface* **2023**, *20*, 20220890. [CrossRef] [PubMed]

41. Büttner, K.; Krieter, J. Illustration of different disease transmission routes in a pig trade network by monopartite and bipartite representation. *Animals* **2020**, *10*, 1071. [CrossRef] [PubMed]

42. Xie, X.; Zhao, L.; Qian, Y. Impact of asymmetric activity on interactions between information diffusion and disease transmission in multiplex networks. *Commun. Theor. Phys.* **2023**, *75*, 075001. [CrossRef]

43. Hearst, S.; Huang, M.; Johnson, B.; Rummells, E. Identifying potential super-spreaders and disease transmission hotspots using white-tailed deer scraping networks. *Animals* **2023**, *13*, 1171. [CrossRef] [PubMed]

44. Shaw, A.K.; White, L.A.; Michalska-Smith, M.; Borer, E.T.; Craft, M.E.; Seabloom, E.W.; Snell-Rood, E.C.; Travisano, M. Lessons from movement ecology for the return to work: Modeling contacts and the spread of COVID-19. *PLoS ONE* **2021**, *16*, e0242955. [CrossRef]

45. Silva, T.C.; Anghinoni, L.; Zhao, L. Quantitative Analysis of the Effectiveness of Public Health Measures on COVID-19 Transmission. *medRxiv* **2020**. Available online: https://www.medrxiv.org/content/10.1101/2020.05.15.20102988v1.full.pdf+html (accessed on 1 August 2024).

46. Gayawan, E.; Awe, O.O.; Oseni, B.M.; Uzochukwu, I.C.; Adekunle, A.; Samuel, G.; Eisen, D.P.; Adegboye, O.A. The spatio-temporal epidemic dynamics of COVID-19 outbreak in Africa. *Epidemiol. Infect.* **2020**, *148*, e212. [CrossRef]

47. Chan, C.H.; Wen, T.H. Revisiting the Effects of High-Speed Railway Transfers in the Early COVID-19 Cross-Province Transmission in Mainland China. *Int. J. Environ. Res. Public Health* **2021**, *18*, 6394. [CrossRef] [PubMed]

48. Dlamini, W.M.D.; Simelane, S.P.; Nhlabatsi, N.M. Bayesian network-based spatial predictive modelling reveals COVID-19 transmission dynamics in Eswatini. *Spat. Inf. Res.* **2021**, *30*, 183–194. [CrossRef]

49. Pribadi, D.O.; Saifullah, K.; Putra, A.S.; Nurdin, M.; Iman, L.O.S.; Rustiadi, E. Spatial analysis of COVID-19 outbreak to assess the effectiveness of social restriction policy in dealing with the pandemic in Jakarta. *Spat. -Spatio-Temporal Epidemiol.* **2021**, *39*, 100454. [CrossRef] [PubMed]

50. Abuhasel, K.A.; Khadr, M.; Alquraish, M.M. Analyzing and forecasting COVID-19 pandemic in the Kingdom of Saudi Arabia using ARIMA and SIR models. *Comput. Intell.* **2020**, *38*, 770–783. [CrossRef] [PubMed]

51. Alboaneen, D.; Pranggono, B.; Alshammari, D.; Alqahtani, N.; Alyaffer, R. Predicting the epidemiological outbreak of the coronavirus disease 2019 (COVID-19) in Saudi Arabia. *Int. J. Environ. Res. Public Health* **2020**, *17*, 4568. [CrossRef] [PubMed]

52. Elhassan, T.; Gaafar, A. Mathematical Modeling of the COVID-19 Prevalence in Saudi Arabia. *medRxiv* **2020**. Available online: https://www.medrxiv.org/content/10.1101/2020.06.25.20138602v1 (accessed on 1 August 2024).

53. Komies, S.; Aldhahir, A.M.; Almehmadi, M.; Alghamdi, S.M.; Alqarni, A.; Oyelade, T.; Alqahtani, J.S. COVID-19 Outcomes in Saudi Arabia and the UK: A Tale of Two Kingdoms. *medRxiv* **2020**. Available online: https://www.medrxiv.org/content/10.1101/2020.04.25.20079640v1 (accessed on 1 August 2024).

54. Khoj, H.; Mujallad, A.F. Epidemic Situation and Forecasting if COVID-19 in Saudi Arabia Using SIR Model. Technical Report. 2020. Available online: https://www.medrxiv.org/content/10.1101/2020.05.05.20091520v1 (accessed on 1 August 2024).

55. Awwad, F.A.; Mohamoud, M.A.; Abonazel, M.R. Estimating COVID-19 cases in Makkah region of Saudi Arabia: Space-time ARIMA modeling. *PLoS ONE* **2021**, *16*, e0250149. [CrossRef]

56. Al-Turaiki, I.; Almutlaq, F.; Alrasheed, H.; Alballa, N. Empirical Evaluation of Alternative Time-Series Models for COVID-19 Forecasting in Saudi Arabia. *Int. J. Environ. Res. Public Health* **2021**, *18*, 8660. [CrossRef]

57. Ministry of Health Saudi Arabia. COVID-19 Dashboard: Saudi Arabia. 2022. Available online: https://covid19.moh.gov.sa/ (accessed on 1 November 2021).

58. Networkx Network Analysis in Python. Networkx Documentation. 2021. Available online: https://networkx.github.io (accessed on 1 August 2024).

59. Gephi. Gephi—The Open Graph Viz Platform. 2021. Available online: https://gephi.org (accessed on 1 August 2024).